

## Remarks

In the Office Action dated May 17, 2005, claims 49-66, in the above-identified U.S. patent application were rejected. Reconsideration of the rejections is respectfully requested in view of the above amendments and the following remarks. Claims 49-66 remain in this application and claims 1-48 have been canceled.

Claim 49 was rejected under 35 USC §103(a) as obvious over Celeste, Ben-Bassat, and Hirel in view of Georgiou further in view of Thompson and Tonouchi. Applicants respectfully point out that the Pro-MP52 according to the present claims cannot be achieved by the process suggested in the office action. A pure composition according to the present invention is possible because proteins with Ala or Met-Ala at the N-terminus are not expressed. It is known that an incomplete cleavage of methionine is achieved when treating with MAP under both *in vitro* and *in vivo* conditions. Thus, if aminopeptidases are used after expression the cleavage would be incomplete even when an excess amount of aminopeptidases is used and thus the preparation would not have the desired homogeneity and the required purity. Even with the help of aminopeptidases, a Pro-MP52 can never be obtained which is in fact free of proteins having an Ala or Met-Ala at the N-terminus. In addition, in such a preparation, aminopeptidases would be present along with the protein. Aminopeptidases are impurities which would be undesirable in a medicament. A complete separation of aminopeptidases, which had previously been added, would not be possible.

Thus, the isolated protein of the present invention would not be obtained by the method suggested in the office action.

As discussed above, even after treatment with aminopeptidases there would still be proteins with an Ala or a Met-Ala at the N-terminus present. The presence of non-native N-terminal methionine in recombinant pharmaceutical proteins can lead to problems. Applicants point out that a difference in one methionine residue at the N-terminal end is known to change the mobility of proteins in RP-HPLC and SDS-PAGE. Differences have been reported for recombinant ricin A chain and interleukin-2. This type of heterogeneity among the protein molecules can cause difficulties in the purification and characterization of these proteins and heterogeneity decreases the yield of pure products. In addition, an extra methionine at the N-terminal end of the protein can affect the biological activity and function of the protein, can alter its stability, and can make it immunogenic when administered as a therapeutic product. The recent debate on whether methionine-free human growth hormone (produced by Eli Lilly and Company) is superior to methionylated human growth hormone (produced by Genentech) exemplifies the importance of this issue. Applicants also point out that the methionine at the N-terminal end is labile to oxidation during the purification process, especially when treated at high pH and under aerobic conditions. Oxidation of the methionine residue to sulfonyl methionine can increase the immunogenicity of the protein.

In addition to the above discussed disadvantages, when using aminopeptidases, it can be assumed that the aminopeptidase preparations

themselves had been isolated and purified and thus there is a risk that they are contaminated with further proteases which have similar purification properties. These contaminated proteases could attack the MP52 protein under favorable reaction conditions (30°C and/or 37°C overnight for the MAP).

When MP52 proteins are present as Met-Ala-Pro-MP52, under realistic conditions in a manufacturing process, when using reaction conditions for aminopeptidases, a large part of the N-termini of Met-Ala-Pro-MP52 would not be accessible to the MAP due to precipitations/aggregations. An *in vitro* treatment of proteins and thus also of Met-Ala-Pro-MP52 with aminopeptidases requires the use of pH values around the physiologic range, i.e. around pH 7. The maintenance of particular pH ranges is important for enzymatic reactions so that an enzyme can work efficiently. The pH profile for the MAP from E.coli can be gathered from Figure 5 of the article Klein et al. (2003). The requirements necessary for the aminopeptidase reaction (pH value about 7.5) are very problematic for the MP52 proteins. MP52, in contrast to the aminopeptidase, is a highly hydrophobic enzyme, which, accordingly, has a very poor solubility under physiologic conditions around a neutral pH value in an aqueous solution. Applicants point out WO 03/043673 which deals with the homogeneous loading of carrier materials with 13MPs, especially human GDF-5 (MP52) in order to obtain devices with osteoinductive properties. Also for the loading of carrier materials, it is important that the protein remains in the solution as long as possible (cf. e.g. page 5, last sentence in the last-but-one paragraph: "An important precondition for this process is a sufficient solubility of the proteins in

the coating solution." or on page 6, bottom: "(a) providing a solution comprising dissolved osteoinductive protein and a buffer which keeps said protein dissolved... "). As described in this application, it is very important to keep a stable, suitably low pH value. A carrier material such as CaP effects an increase of the pH value which must be avoided by a buffer since otherwise aggregations/precipitations arise (cf. page 7, middle until page 8, middle). The pH-dependent solubility of human GDF-5 (MP52) is shown in Example 3 and Figures 1 and 2. It is shown that GDF-5 is only soluble in an acid range (pH 5) or in the alkalic range (pH > 10). In the pH range between 6.0 and 9.5 (this pH range is, as explained above, necessary for the aminopeptidase reaction) only an extremely low solubility is shown (< 5pg/ml) (cf. page 22, last two sentences under Example 3).

MP52 has an extremely poor solubility under conditions wherein the enzymatic reaction of aminopeptidases takes place. Under conditions where MP52 is soluble, the MAP cannot work or can work only very inefficiently. Thus, in a manufacturing process and at the conditions for an aminopeptidase treatment, micro-precipitations and aggregations of MP52 will always occur. With such an aggregation/precipitation it must be assumed that a part of the N-termini of Met-Ala-Pro-MP52 will not be accessible to the MAP due to physical reasons, completely independent from the amount or the excess of MAP used. With regard to these N-termini it is reasonable to assume that a cleavage of Met would not be affected. In any case, one skilled in the art would not subject MP52 to conditions suitable for MAP since it is known that precipitations and micro-

precipitations, as they occur due to poor solubility, lead to a partial or complete inactivation (cf. page 6, lines 4-5: "Moreover, it is to be understood that the osteoinductive proteins are not aggregated and partially or entirely inactivated due to precipitation or micro-precipitation..."). The 3-dimensional folding of the proteins changes due to precipitation.

Tonouchi does not make any statements regarding the pH-value but refers to an article of Yaron (1971). Yaron indicates that the optimal pH value is at 8.6 (last sentence, page 529). Figure 1 A on page 530 shows the pH profile of aminopeptidase P. At the end of the first paragraph on this page, Yaron states that "This maximum was observed at all pH values at which activity could be tested (7.0-9.2)". The pH range of 7.0-9.2, wherein the activity of aminopeptidase P can be tested, is always in a range where MP52 has a poor solubility (sufficient solubility of MP52 occurs only above pH 10) and therefore a part of the N-termini of Met-Ala-Pro-MP52 would not be accessible to the MAP.

In view of the above discussion, it is clear that during the treatment of Met-Ala-Pro-MP52 with aminopeptidases, some of the methionine would not be cleaved even when using an excess of MAP. Thus, the Pro-MP52 preparation obtained using the process suggested in the office action would be contaminated with an excess of MAP and aminopeptidase P, with Met-Ala-Pro-MP52 and possibly also with Ala-Pro-MP52. Thus, such a preparation clearly differs from the pure Pro-MP52 preparation according to the present claims.

Applicants also contend that it would not have been obvious from the prior art to produce Pro-MP52 at all. In other words, at the time of the present

invention the skilled artisan would not have been motivated to produce MP52 as a homogeneous material since there is no suggestion in the prior art that Pro-MP52 could be obtained in a homogeneous form and that it would not be further decomposed by aminopeptidases. The use of aminopeptidases would lead to totally different mixed products and not to homologously isolated proteins as in claim 49. In view of the above discussion, applicants request that this rejection be withdrawn.

Claims 49 and 50 were rejected under 35 USC §103(a) as obvious over Celeste, Ben-Bassat, and Hirel in view of Georgiou further in view of Thompson and Tonouchi and further in view of Hötten and Cerletti. Claims 49-60, 63 and 66 were rejected under 35 USC §103(a) as obvious over Celeste, Ben-Bassat, and Hirel in view of Georgiou further in view of Thompson and Tonouchi and further in view of Hötten and Cerletti and Neidhardt. Claims 49-51, 64, 65 and claims 52-60, 63 and 66 were rejected under 35 USC §103(a) as obvious over Celeste, Ben-Bassat, and Hirel in view of Georgiou further in view of Thompson and Tonouchi and further in view of Hötten and Cerletti and Neidhardt further in view of Hötten A and Chen. Claims 49-51, 61 and 62 were rejected under 35 USC §103(a) as obvious over Celeste, Ben-Bassat, and Hirel in view of Georgiou further in view of Thompson and Tonouchi and further in view of Hötten and Cerletti and Neidhardt further in view of Ron and Avis. Claims 49-51 and 60 were rejected under 35 USC §103(a) as obvious over Celeste, Ben-Bassat, and Hirel in view of Georgiou further in view of Thompson and Tonouchi and further in view of Hötten and Cerletti and Neidhardt further in view of Oppermann. As


discussed above, a homogeneous Pro-MP52 cannot be obtained when aminopeptidases are used because the enzymes are not 100% efficient. Therefore, applicants contend that the limitation in claim 49 that proteins according to SEQ ID NO:1 with either a) an ala or b) a Met-Ala at the N-terminus are not expressed or present distinguish the claimed invention from the cited prior art. In view of the above discussion applicants request that these rejections be withdrawn.

Claims 49-66 were rejected under the judicially created doctrine of obviousness type double patenting as unpatentable over claims 1-7 of copending application no. 10/365,231. A terminal disclaimer is being prepared and will be filed shortly.

Applicants respectfully submit that all of claims 49-66 are now in condition for allowance. If it is believed that the application is not in condition for allowance, it is respectfully requested that the undersigned attorney be contacted at the telephone number below.

In the event this paper is not considered to be timely filed, the Applicant respectfully petitions for an appropriate extension of time. Any fee for such an extension together with any additional fees that may be due with respect to this paper, may be charged to Counsel's Deposit Account No. 02-2135.

Respectfully submitted,

By \_\_\_\_\_

Monica Chin Kitts  
Attorney for Applicants  
Registration No. 36,105  
ROTHWELL, FIGG, ERNST & MANBECK, p.c.  
Suite 800, 1425 K Street, N.W.  
Washington, D.C. 20005  
Telephone: (202)783-6040



## Protonation States of Methionine Aminopeptidase and Their Relevance for Inhibitor Binding and Catalytic Activity\*<sup>§</sup>

Received for publication, May 21, 2003, and in revised form, July 31, 2003  
Published, JBC Papers in Press, September 26, 2003, DOI 10.1074/jbc.M305325200

Christian D. P. Klein<sup>‡§</sup>, Rolf Schiffmann<sup>‡</sup>, Gerd Folkers<sup>||</sup>, Stefano Pianal<sup>||</sup>,  
and Ursula Röthlisberger<sup>||</sup>

From the <sup>‡</sup>FR 8.5 Pharmazeutische und Medizinische Chemie, Saarland University, D-66041 Saarbrücken, Germany,  
<sup>||</sup>Department of Chemistry and Applied Biosciences, Pharmaceutical Chemistry, Swiss Federal Institute of Technology,  
Winterthurerstrasse 190, CH-8057 Zürich, Switzerland, and <sup>||</sup>Swiss Federal Institute of Technology,  
Institute of Molecular and Biological Chemistry, CH-1015 Lausanne, Switzerland

We have performed a computational study of different protomeric states of the methionine aminopeptidase active site using a combined quantum-mechanical/molecular mechanical simulation approach. The aim of this study was to clarify the native protonation state of the enzyme, which is needed for the development of novel irreversible inhibitors that can possibly be used as antiangiogenic and antibiotic drugs by virtual screening and other drug design methods. The results of the simulations indicated that two protonation states are possible without disturbing the overall geometry of the active site. We then verified experimentally the presence of the two protonation states by studying the substrate hydrolysis and inhibitor binding reactions at different pH values and come to the conclusion that one of the protomeric states is relevant for inhibitor binding, whereas the other is relevant for substrate hydrolysis. This result has implications for the development of other inhibitors of this class of enzymes and adds a new perspective to the pharmacological properties of the antiangiogenic drug fumagillin, which is an irreversible inhibitor of the human methionine aminopeptidase type II.

Methionine aminopeptidases (MetAPs)<sup>1</sup> play a central role for *in vivo* protein synthesis as they remove the starter methionine from newly synthesized proteins. The natural product fumagillin, an epoxide, covalently modifies one of the active-site histidines in the eukaryotic methionine aminopeptidase II (MetAP-II) (1–4) and other MetAPs (*cf.* Fig. 1). Fumagillin inhibits the growth of vessels in tumors, and a derivative of the compound has been evaluated in clinical trials as an anticancer drug. The antiangiogenic effect of fumagillin and other inhibitors of MetAP-II have been attributed to the inhibition of the Ets-1 transcription factor expression and the activation of the

p53 pathway (5, 6). Besides from being anticancer drug targets, MetAPs have the potential to become the target proteins of antibacterial substances because the MetAP functionality is essential for cell growth and bacteria possess only one of the two known MetAP subtypes (7).

MetAPs are metal-dependent enzymes. It is not clear which metal activates the MetAPs *in vivo*. For *in vitro* experiments, cobalt is commonly used because it activates all known MetAPs and the cobalt-substituted enzymes are usually the most active (8). Zinc and iron(II) have also been shown to activate some MetAPs (9, 10). The metal-chelating residues in all known MetAPs are two glutamates, two aspartates, and one histidine. The geometric arrangement of these residues is practically identical in all of the MetAP x-ray structures (11, 12). Several three-dimensional structures of MetAPs have been determined by x-ray diffraction methods including the structure of human MetAP-II with a covalently bound fumagillin molecule (13–15).

Density functional theory (16, 17) has long been used to study the reactivity of organic molecules and recently began to find its way into biochemistry (18). We present here an example in which the application of density functional theory to a biochemical problem led to a hypothesis, which was subsequently verified by experiments. Our results do not only explain a couple of biochemical phenomena related to MetAPs but also demonstrate the impact that modern quantum-chemical methods can have on the study of biological systems where they can help fill the gap between mere conjectures and physical reality.

Our motivation for examining the MetAPs from a theoretical point of view stems from the highly selective, irreversible inhibition mechanism of fumagillin and related epoxides. Many enzyme inhibitors that form a covalent adduct with their target proteins (*e.g.* the  $\beta$ -lactam antibiotics and acetyl salicylic acid) are important drugs. We believe that the fumagillin/MetAP example is a good test case for theoretical methods that aim at rationalizing the development of covalent enzyme inhibitors, because a large amount of high quality x-ray structural data, also with bound inhibitors, has been published over the last few years.

As a first step toward an understanding of the catalytic and inhibitor-binding mechanisms of MetAPs, we studied different protonation states of the active site water molecules by means of molecular dynamics simulations in a combined quantum-mechanical/molecular-mechanical (QM/MM) framework. In the 1.9-Å resolution, x-ray structure of *Escherichia coli* MetAP (Protein Data Bank code 2mat), one water molecule (or hydroxide ion) is bridging the two cobalt ions and another water molecule is bound to the cobalt ion that is not coordinated to the histidine. Three different protomeric states were examined (see

\* The costs of publication of this article were defrayed in part by the payment of page charges. This article must therefore be hereby marked "advertisement" in accordance with 18 U.S.C. Section 1734 solely to indicate this fact.

<sup>§</sup> The on-line version of this article (available at <http://www.jbc.org>) contains Supplemental data.

<sup>§</sup> To whom correspondence should be addressed: FR 8.5 Pharmazeutische und Medizinische Chemie, Saarland University, D-66041 Saarbrücken, Germany. Tel.: 49-681-302-2924; Fax: 49-681-302-4386; E-mail: [cdpk@mx.uni-saarland.de](mailto:cdpk@mx.uni-saarland.de).

<sup>1</sup> The abbreviations used are: MetAP, methionine aminopeptidases; MetAP-II, methionine aminopeptidase II; QM, quantum-mechanical; MM, molecular-mechanical; CPMD, Car-Parrinello Molecular Dynamics; MD, Molecular Dynamics; HOMO, highest occupied molecular orbital.

Fig. 2) as follows: one with two bound water molecules, one with a bridging hydroxide ion and a water molecule, and one with two hydroxide ions. For the quantum-mechanical part of the system, the *ab initio* molecular dynamics method described by Car and Parrinello (CPMD) (19) was used. Because an accurate treatment of the open-shell cobalt(II) ion is very demanding in the framework of CPMD, we decided to use zinc(II) ions as the active-site metals in the CPMD simulations. The fundamental problem with cobalt is the uncertainty of its spin state and the multiplicity of the bi-cobalt system. A computational study of a di-cobalt system would therefore require the simulation of eight different electronic configurations that is not feasible with CPMD and currently available supercomputer resources. Given the fact that at least some MetAPs have been shown to be active with zinc and considering that a thorough theoretical analysis of the zinc- and cobalt-substituted truncated MetAP active sites did not reveal major geometrical differences between a di-zinc and a di-cobalt system (20), we assume that the replacement of cobalt by zinc does not affect the validity of our results. Furthermore, preliminary CPMD simulations on a di-cobalt MetAP active site with one water and one hydroxide ion did not show geometric or dynamic differences to a di-zinc system (see Supplemental data).

#### EXPERIMENTAL PROCEDURES

**Theoretical Methods**—The density functional theory-based Car-Parrinello (19) molecular dynamics program CPMD, version 3.5, was used for the QM/MM simulations of MetAP (21–24). AMBER94 force-field parameters were used for the MM part (25, 26). All of the systems were

fully hydrated with TIP3P (three-point transferable intermolecular potential) water molecules in a periodic box and equilibrated by extensive classical-mechanical molecular dynamics (MD) simulations with AMBER94 prior to the *ab initio* MD simulations. Visualization was done with VMD (27). The quantum parts included the five metal-binding amino acids (truncated to acetate ions and imidazole, respectively; free valences were capped by adding hydrogen atoms), the two zinc ions, and the two water/hydroxide molecules coordinating to them. The QM parts were minimized (annealed to a temperature below 0.1 K) before the start of the production MD phase. CPMD parameters were as follows: isolated system calculations; gradient-corrected exchange-correlation functionals due to Becke (28) and Lee *et al.* (29); plane waves basis set; kinetic energy cutoff: 70 Ry; soft norm-conserving Troullier-Martins (30) pseudopotentials for the core electrons; time step (6 atomic units); Nosé-Hoover thermostat at 300 K, coupling frequency of 500  $\text{cm}^{-1}$ ; and fictitious electron mass (800 a.u.) (28–32). The size of the orthorhombic QM box was  $13.2 \times 15.9 \times 17.2$  Å, corresponding to a minimum image distance of 6.4 Å. Simulations with cobalt were performed with a kinetic energy cut-off of 90 Ry and Becke (28) and Perdew (33) exchange-correlation functionals (33, 34).

**Experimental Methods**—*E. coli* MetAP was purified from an overproducer strain that was kindly provided by Drs. Lowther and Matthews. Assays were performed in 96-well microtiter plates using the method of Yang *et al.* (35) with Met-Gly-Met-Met as substrate and an enzyme concentration of 12 nM. The fumagillin concentration in the inhibition experiments was 66  $\mu\text{M}$ , which is slightly below the  $\text{IC}_{50}$  of fumagillin at pH 7 under otherwise identical conditions. Tris/maleate buffer was used for the incubation of MetAP with and without fumagillin at pH 5–8.5 (volume of 30  $\mu\text{l}$ , 15 min, 37 °C). For the ensuing Met-Gly-Met-Met hydrolysis and detection reactions, the pH was adjusted to pH 7.5 by adding 170  $\mu\text{l}$  of 4-fold concentrated Tris/maleate buffer. The fluorescent reaction product (resorufin) was measured using a Wallac microtiter plate reader. All of the experiments were performed in triplicate. Detailed descriptions of the experiments are given in Supplemental material.

#### RESULTS

**Simulations**—In the CPMD simulations, the system with the two water molecules coordinated to the zinc ions showed a pronounced movement of the coordinating water molecules away from the x-ray structure of *E. coli* MetAP that has one water molecule located between the metals. The system evolved to a structure in which there was no more “bridge” between the metals and one water molecule started to form a strong hydrogen bond to a carboxylic acid. The simulation was stopped after ~5000 steps of simulation (0.85 ps), because the geometry remained essentially stable. In contrast, the structure with one bridging hydroxide was stable during the whole simulation time (~10,000 steps), showing only the expected thermal motions and a twist of one carboxylic acid group. Fig. 3 gives a comparison of the active site geometries of the bi-water and the water-hydroxide system with the crystal structure. Hydrogens have been omitted for clarity. The final state of the bi-hydroxide system is not shown, because it deviates strongly from the crystal structure and a comparison with the other systems would not make any sense. After only ~1000

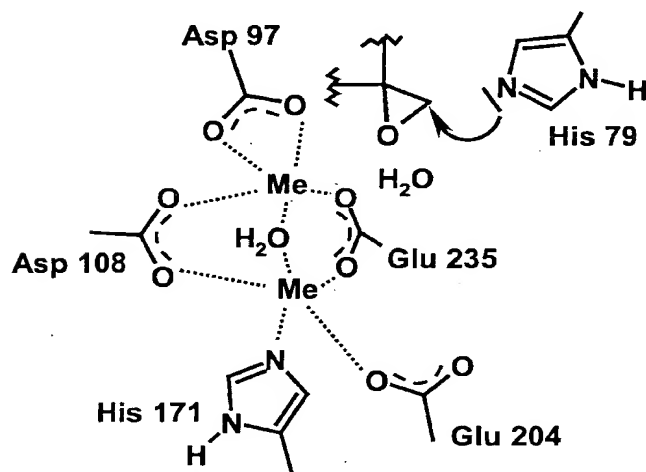


FIG. 1. Binding of fumagillin in the MetAP active site. Me, metal ion. The numbering is for *E. coli* MetAP.

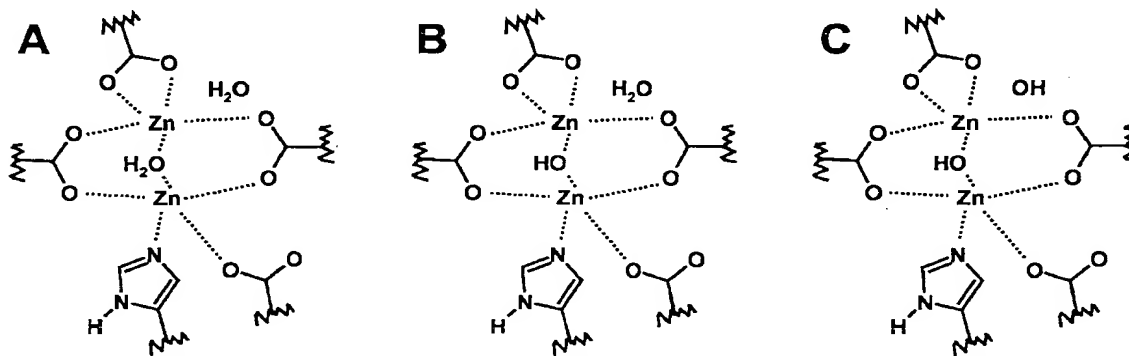


FIG. 2. A–C, the three different protomeric states for which CPMD simulations were performed.

FIG. 3. Final structures of the CPMD simulations of the bi-water and the water-hydroxide systems in comparison with the x-ray structure. Hydrogens and the surrounding residues of the enzyme are not shown for clarity. The x-ray-structure is shown in CPK (Corey-Pauling-Koltun) colors, the bi-water system in yellow and the water-hydroxide system is in green. Me, metal ion; Wat, water.

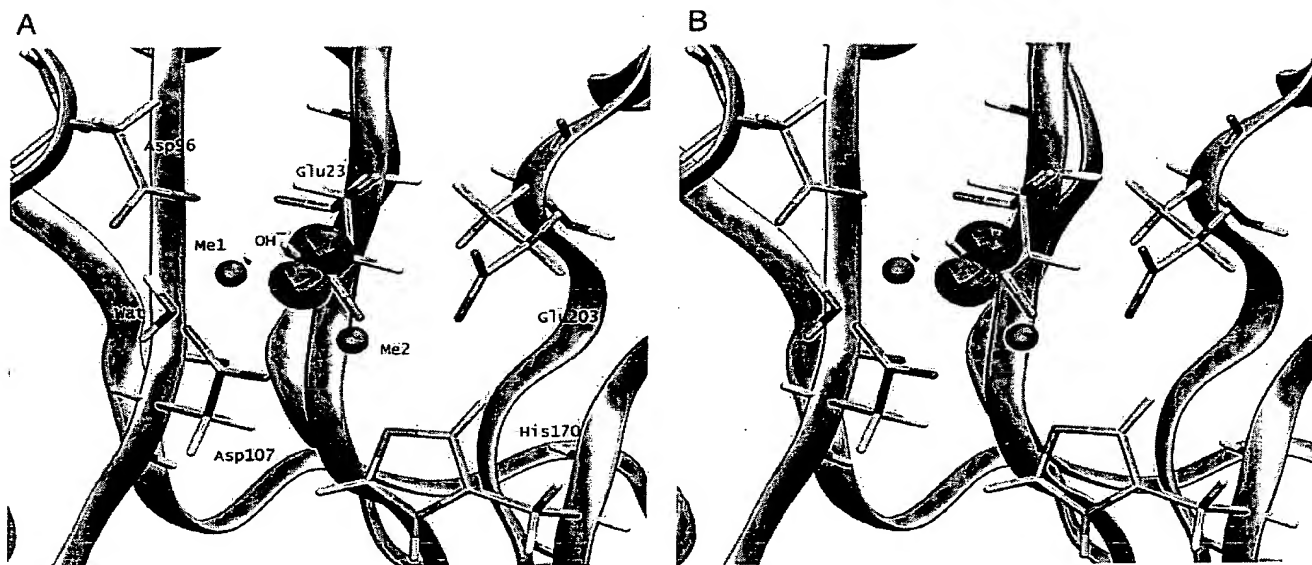
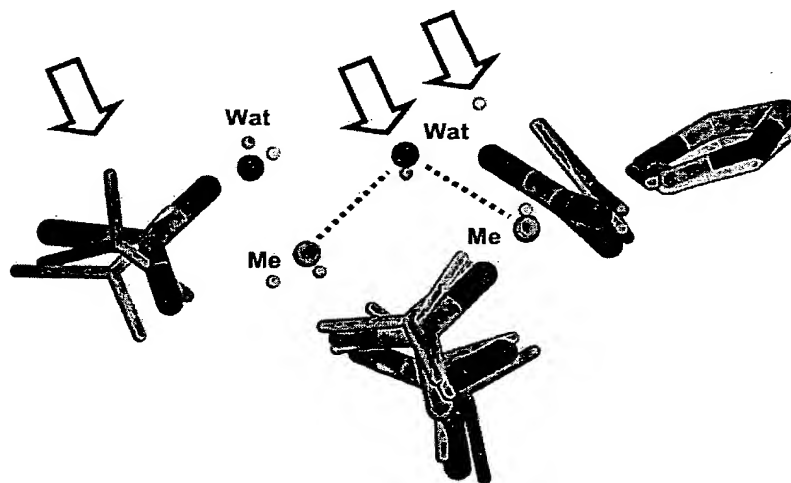


FIG. 4. Final structure of the active site with one hydroxide ion and one water molecule coordinated to the metals (Me1, Me2, purple spheres). The HOMO-1 orbital located at the bridging hydroxide ion is also shown (red and blue clouds). The cut-off for the visualization of the HOMO-1 electron density was  $0.1 \text{ e/au}^3$  (electron per cubic atomic units).

steps of simulation, large deviations from the crystal structure were observed in the bi-hydroxide system. After 3000 steps, the metal-coordinating residues were considerably displaced from the crystal structure positions and the simulation was stopped.

It becomes clear from Fig. 3 that both the bi-water and the water-hydroxide system are intrinsically stable and quite similar to the 2mat x-ray structure. The root mean square deviations of the active site heavy atoms in comparison with the x-ray structure (hydrogens were not used because they are not present in the x-ray structure) are  $0.81 \text{ \AA}$  for the bi-water and  $0.85$  for the water-hydroxide system. The main changes are as follows. 1) The bridging water leaves the position between the two metals in the bi-water simulation. 2) In the water-hydroxide simulation, the bridging hydroxide remains in place and one of the metal-coordinating carboxylic acid groups twists to a position that is perpendicular to the x-ray structure. Nevertheless, this residue remains a binding partner for one of the metal ions.

A picture of the final state of the simulation is shown in Fig. 4. This figure also shows the HOMO-1 orbital, which is local-

ized at the hydroxide ion, the species that very likely acts as the nucleophilic agent in the substrate hydrolysis reaction. The HOMO orbital, which is  $\sim 0.5 \text{ eV}$  higher in energy, is localized at one of the carboxylic acid groups.

**Experiments**—The pH profiles of the inhibitor binding and substrate hydrolysis reaction are given in Fig. 5. It is evident that the pH optimum of the substrate hydrolysis reaction is at pH 7.5, whereas the binding of fumagillin becomes increasingly favored at lower pH.

#### DISCUSSION

The results presented above allow the following conclusions. 1) In the x-ray structure of *E. coli* MetAP (2mat), the bridging water molecule is most probably deprotonated. However, an active site with two (fully protonated) water molecules coordinated to the metal ions is also stable, albeit with a different coordination geometry. The x-ray structure of the *E. coli* MetAP (2mat) was determined at a pH larger than 7, whereas several other MetAP structures were determined at a more acidic pH. (human MetAP-II, see Ref. 15). The pH in the crys-

FIG. 5. pH profile for the substrate hydrolysis and fumagillin binding reactions of *E. coli* MetAP (mean values  $\pm$  S.D. and with error bars).

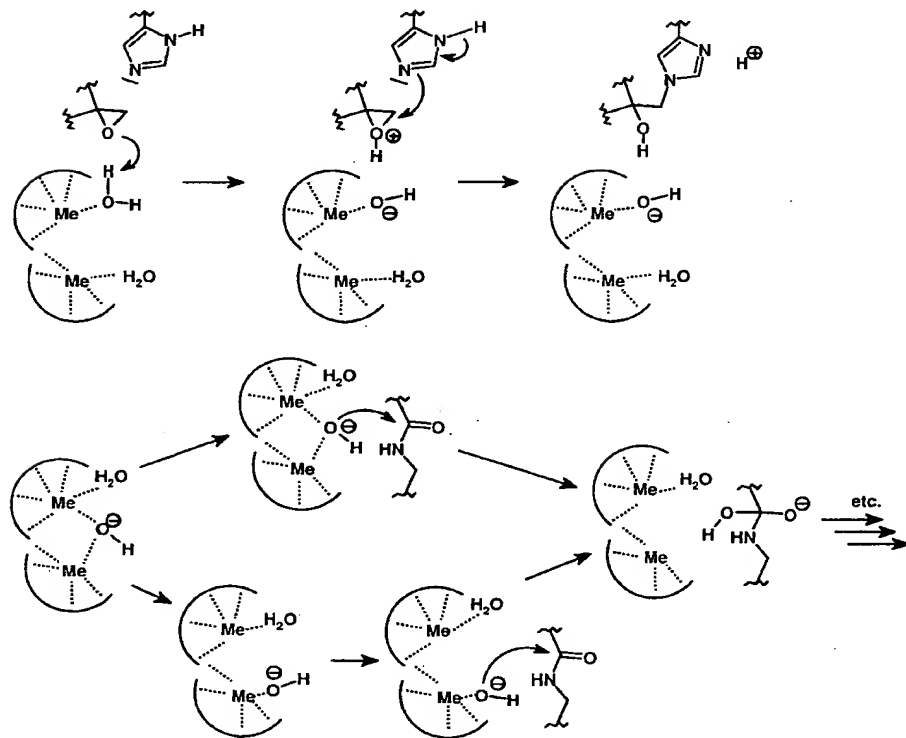
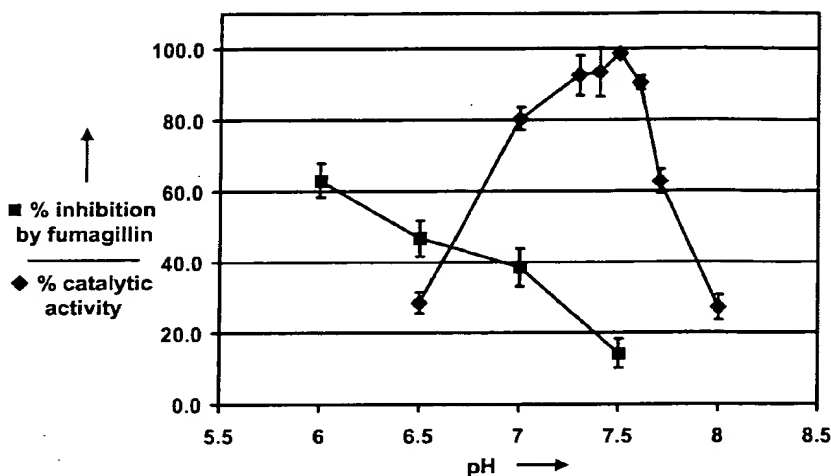


FIG. 6. Mechanisms of the fumagillin binding and substrate hydrolysis reactions in MetAP. Only the initial steps of the substrate hydrolysis are shown (see the literature references in the text for more details regarding the MetAP substrate hydrolysis mechanism).

tallization medium can not be determined exactly, but the experimental (buffer) conditions described by Liu *et al.* (15) indicate that the pH was below 7. Examining one of these x-ray structures (1bn5), we found that no bridging water molecule is present between the two metals. Taken together, the x-ray structure and the results of the CPMD simulations indicate that two protonation states are possible without disrupting the active site geometry. At a more basic pH, one water molecule is deprotonated and bridging the two metal ions. From the electronic structure calculations, this protonation state is expected to be relevant for the catalytic process. Two water molecules are present in the active site at more acidic pH, each one coordinating a different metal ion.

The covalent binding of fumagillin to MetAP requires protonation of the epoxide oxygen. Proton donation from an active site group, in particular from one of the active site water

molecules, is more likely in the protonation state with two water molecules (*i.e.* at more acidic pH).

In other words, our calculations and the analysis of the crystal structure indicate that the active site of binuclear *E. coli* MetAP is characterized by the presence of a water molecule with a  $pK_a$  of  $\sim 7$ . This is at the lower border of the  $pK_a$  values reported for waters coordinating to zinc ions in organic complexes (36). The binding of fumagillin is expected to be favored at more acidic pH, whereas a more basic pH would be required for catalysis. This finding opened the way to an experimental validation of the theory of which we determined the pH-profile of the fumagillin inhibition reaction and the enzymatic activity of MetAP (see Fig. 5). It is obvious that the binding of the inhibitor is favored under more acidic conditions as compared with those that are optimal for the substrate hydrolysis reaction. This observation provides strong substan-

tiation to our interpretation of the QM/MM CPMD simulation results.

In summary, the mechanisms of the fumagillin binding and the initial step of the substrate hydrolysis reactions are shown in Fig. 6. The substrate hydrolysis reaction starts with the attack of the metal-bound hydroxide ion to the carbonyl carbon of the scissile peptide bond. This mechanism differs slightly from the one that is given in the recent literature (12) where the deprotonation of the metal-bridging water occurs after the substrate has been bound in the active site.

Recent theoretical work on the reaction mechanism of imipenem binding to the di-nuclear zinc- $\beta$ -lactamase (37) and the substrate hydrolysis mechanism of the di-nuclear bovine lens leucine aminopeptidase (38) indicate that the nucleophilic attack on the substrate originates from a "terminally" bound and not a bridging hydroxide ion. The nucleophilicity of a hydroxide ion that is complexed to one metal ion is higher than that of a bridging hydroxide. Considering these results, we suggest a mechanism (Fig. 6, bottom) in which a bridging hydroxide (as in the crystal structure) is found in the resting state of the enzyme and the binding of the substrate causes a rearrangement of the complexation pattern. Subsequently, the amide carbonyl carbon is attacked by the terminally bound hydroxide ion, which has an increased nucleophilicity as compared to the bridging hydroxide ion in the resting state.

It may be argued that the acidic pH leads to the protonation of an active site residue other than the metal-coordinating water and that fumagillin binding is therefore facilitated by a modification of the non-covalent complex that precedes the binding reaction. However, the only groups that could readily be protonated within the studied pH range would be His-79 and His-178. His-79 is the binding partner of fumagillin. A protonated and therefore positively charged His-79 would certainly be much less prone to act as a nucleophile on fumagillin, and it can thus be assumed that His-79 remains neutral. Therefore, if one assumes that His-79 is not being protonated, it is also very unlikely that His-178 is protonated because the chemical surrounding (which could influence the  $pK_a$  of the histidine imidazole) is quite similar for both histidines. Furthermore, literature values for the histidine side chain  $pK_a$  range from 6 to 6.4, which is below the value of  $\sim 7$  for the protonation event in the MetAP active site.

The results of the CPMD simulations presented here do not provide quantitative free energy data of the different protonic states. It would certainly be very useful to obtain such data, which could be used to calculate the  $pK_a$  of metal-bound waters and other ionizable groups in the active site. However, one must be aware of the fact that the prediction of  $pK_a$  values would require very exact free energy data of different protonic states and a very complete sampling of conformational space. Even in the classical-mechanical simulation framework (where the computational cost of simulations is smaller by several orders of magnitude and a much more complete exploration of conformational space is possible), free energies are notoriously difficult to predict (39). Thus, we think that a meaningful prediction of free energy differences and  $pK_a$  values by *ab initio* simulation methods is currently not feasible. The situation may be somewhat different when less complex systems such as pure water or small solvated ions are considered. In such cases, present computer capabilities can be sufficient to adequately determine  $pK_a$  values by *ab initio* MD simulations.

Recent experimental work (40) has shown that *E. coli* MetAP may under certain circumstances function as a mononuclear enzyme, i.e. with only one metal ion coordinating to the active site residues. The metal content and the identity of the metal in the MetAP enzymes *in vivo* are not known. With the sole

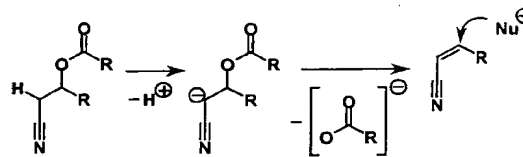


FIG. 7. De-protonation of a  $\beta$ -hydroxynitrile ester, subsequent ester hydrolysis, and formation of acrylonitrile. Acrylonitrile then binds to nucleophiles in the active site, e.g. histidine or cysteine residues.

exception of the publication mentioned above, all of the experimental data of *E. coli* and yeast and human MetAPs, including all of the published x-ray structures, have been obtained with bi-nuclear enzymes because enzymes with lower metal content had only marginal or no catalytic activity under the respective experimental conditions. Therefore, we are confident that it is reasonable to assume the presence two metal ions in the active site as we did in our simulation system.

Fumagillin and its congeners inhibit the growth of vessels in tumors. Considering the fact that the extracellular pH in tumors is more acidic than in normal tissues, (41) and assuming that the endothelial cells of vessels in tumors are under the influence of the acidic extracellular tumor pH, one may reason that the pH profile of the fumagillin-MetAP binding reaction leads to selectivity (or targeting) of the fumagillin effect to tumor vessels.

The results presented here have several implications for the rational design of MetAP inhibitors. First, virtual screening (docking/scoring) procedures should preferably be made on MetAP active sites with a net charge of  $-1$  if inhibition at neutral pH is desired (e.g. for MetAP inhibitors with antibacterial activity). The active site net charge has a pronounced influence on the binding energetics of ligands in virtual screening and in physical reality, because electrostatic interactions are the strongest driving force for intermolecular attraction and repulsion. Second, irreversible inhibitors different from fumagillin should preferably be compounds that are activated by a nucleophilic attack (coming from the hydroxide ion) or by deprotonation. Such inhibitors would be much more active at physiological pH than fumagillin. For instance, the deprotonation of  $\beta$ -hydroxynitrile esters (cf. Fig. 7) causes cleavage of the ester bond and subsequent formation of acrylonitrile, which can then bind (as a "Michaelis-like" electrophile) to one of the cysteine residues near the MetAP active site. The sequence of reactions would be based on a "basic activation" and not acidic activation as with fumagillin.

In conclusion, we have clarified the protonation behavior of the MetAP active site and made an experimental proof of a hypothesis that was generated on the basis of quantum-mechanical calculations.

**Acknowledgments**—We thank Prof. R. Hartmann at Saarland University for continued support for this project and the Deutsche Forschungsgemeinschaft for financial support to C. Klein (KL 1356). CSCS in Manno, Switzerland and HLRS in Stuttgart, Germany kindly provided CPU time for this project. The group of Prof. R. Bernhard at the University of the Saarland helped with the expression of *E. coli* MetAP from a strain that was kindly provided by Profs. B. Matthews and W. T. Lowther. We are also grateful to one of the reviewers, who suggested us to consider a terminally bound hydroxide ion as the nucleophilic species in the substrate hydrolysis reaction.

#### REFERENCES

- Ingber, D., Fujita, T., Kishimoto, S., Sudo, K., Kanamaru, T., Brem, H., and Folkman, J. (1990) *Nature* 348, 555–557.
- Griffith, E. C., Su, Z., Turk, B. E., Chen, S., Chang, Y. H., Wu, Z., Biemann, K., and Liu, J. O. (1997) *Chem. Biol.* 4, 461–471.
- Sin, N., Meng, L., Wang, M. Q. W., Wen, J. J., Bornmann, W. G., and Crews, C. M. (1997) *Proc. Natl. Acad. Sci. U. S. A.* 94, 6099–6103.
- Griffith, E. C., Su, Z., Niwayama, S., Ramsay, C. A., Chang, Y. H., and Liu, J. O. (1998) *Proc. Natl. Acad. Sci. U. S. A.* 95, 15183–15188.

5. Wernert, N., Stanjek, A., Kiriakidis, S., Hügel, A., Jha, H. C., Mazitschek, R., and Giannis, A. (1999) *Angew. Chem. Int. Ed. Engl.* **38**, 3228–3231
6. Zhang, Y., Griffith, E. C., Sage, J., Jacks, T., and Liu, J. O. (2000) *Proc. Natl. Acad. Sci. U. S. A.* **97**, 6427–6432
7. Li, X., and Chang, Y. H. (1995) *Proc. Natl. Acad. Sci. U. S. A.* **92**, 12357–12361
8. Ben-Bassat, A., Bauer, K., Chang, S. Y., Myambo, K., Boosman, A., and Chang, S. (1987) *J. Bacteriol.* **169**, 751–757
9. D'Souza, V. M., and Holz, R. C. (1999) *Biochemistry* **38**, 11079–11085
10. Walker, K. W., and Bradshaw, R. A. (1998) *Protein Sci.* **7**, 2684–2687
11. Lowther, W. T., and Matthews, B. W. (2000) *Biochim. Biophys. Acta* **1477**, 157–167
12. Lowther, W. T., and Matthews, B. W. (2002) *Chem. Rev.* **102**, 4581–4608
13. Roderick, S. L., and Matthews, B. W. (1993) *Biochemistry* **32**, 3907–3912
14. Lowther, W. T., Orville, A. M., Madden, D. T., Lim, S., Rich, D. H., and Matthews, B. W. (1999) *Biochemistry* **38**, 7678–7688
15. Liu, S., Widom, J., Kemp, C. W., Crews, C. M., and Clardy, J. (1998) *Science* **282**, 1324–1327
16. Kohn, W., and Sham, J. (1965) *Phys. Rev. A* **140**, 1133–1138
17. Hohenberg, P., and Kohn, W. (1964) *Phys. Rev. B* **136**, 864–871
18. Carloni, P., Rothlisberger, U., and Parrinello, M. (2002) *Acc. Chem. Res.* **35**, 455–464
19. Car, R., and Parrinello, M. (1985) *Phys. Rev. Lett.* **55**, 2471–2474
20. Jorgensen, A. T., Norrby, P.-O., and Liljefors, T. (2002) *J. Comput. Aided Mol. Des.* **16**, 167–179
21. Hutter, J., Alavi, A., Deutsch, T., Bernasconi, M., Goedecker, S., Marx, D., Tuckerman, M., and Parrinello, M. (1995–2003) *CPMD*, Max-Planck Institute für Festkörperforschung, Stuttgart, Germany and IBM Zürich Research Laboratory, Zürich, Switzerland
22. Laio, A., VandeVondele, J., and Rothlisberger, U. (2002) *J. Chem. Phys.* **116**, 6941–6947
23. Laio, A., VandeVondele, J., and Rothlisberger, U. (2002) *J. Phys. Chem. B* **106**, 7300–7307
24. Colombo, M. C., Guidoni, L., Laio, A., Magistrato, A., Maurer, P., Piana, S., Rohrig, U., Spiegel, K., Sulpizi, M., VandeVondele, J., Zumstein, M., and Rothlisberger, U. (2002) *Chimia* **56**, 11–17
25. Cornell, W. D., Cieplak, P., Bayly, C. I., Gould, I. R., Merz, K. M., Ferguson, D. M., Spellmeyer, D. C., Fox, T., Caldwell, J. W., and Kollman, P. A. (1995) *J. Am. Chem. Soc.* **117**, 5179–5197
26. Case, D. A., Pearlman, D. A., Caldwell, J. W., Cheatham III, T. E., Ross, W. S., Simmerling, C. L., Darden, T. A., Merz, K. M., Stanton, R. V., Cheng, A. L., Vincent, J. J., Crowley, M., Tsui, V., Radmer, R., Duan, Y., Pitera, J., Massova, I., Seibel, G. L., Singh, U. C., Weiner, P., and Kollman, P. A. (1999) *AMBER6*, University of California, San Francisco, CA
27. Humphrey, W., Dalke, A., and Schulten, K. (1996) *J. Mol. Graph.* **14**, 33–38
28. Becke, A. D. (1988) *Phys. Rev. A* **38**, 3098–3100
29. Lee, C. L., Yang, W., and Parr, R. G. (1988) *Phys. Rev. B* **37**, 785–789
30. Troullier, N., and Martins, J. L. (1991) *Phys. Rev. B* **43**, 1993–2006
31. Nose, S. (1984) *Mol. Phys.* **52**, 255–268
32. Barnett, R. N., and Landman, U. (1993) *Phys. Rev. B* **48**, 2081–2097
33. Perdew, J. P. (1986) *Phys. Rev. B* **33**, 8822–8824
34. Rovira, C., Kunc, K., Hutter, J., and Parrinello, M. (2001) *Inorg. Chem.* **40**, 11–17
35. Yang, G., Kirkpatrick, R. B., Ho, T., Zhang, G. F., Liang, P. H., Johanson, K. O., Casper, D. J., Doyle, M. L., Marino, J. P., Thompson, S. K., Chen, W. F., Tew, D. G., and Meek, T. D. (2001) *Biochemistry* **40**, 10645–10654
36. Bertini, I., and Luchinat, C. (1994) in *Bioinorganic Chemistry* (Bertini, I., Gray, H. B., Lippard, S. J., and Valentine, J. S., eds), pp. 37–106, University Science Books, Sausalito, CA
37. Suarez, D., Diaz, N., and Merz, K. M., Jr. (2002) *J. Comput. Chem.* **23**, 1587–1600
38. Schürer, G., Horn, A. H. C., Gedeck, P., and Clark, T. (2002) *J. Phys. Chem. B* **106**, 8815–8830
39. Reinhardt, W. P., Miller, M. A., and Amon, L. M. (2001) *Acc. Chem. Res.* **34**, 607–614
40. Cosper, N. J., D'souza, V. M., Scott, R. A., and Holz, R. C. (2001) *Biochemistry* **40**, 13302–13309
41. Gillies, R. J., Raghunand, N., Karczmar, G. S., and Bhujwala, Z. M. (2002) *J. Magn. Reson. Imaging* **16**, 430–450

The  $K_m$  values of the different *p*-nitroanilides are as follows: glycine 1.75 mM, phenylalanine 3.2, alanine 0.6, leucine 0.24 mM (measured at pH 7 in 0.06 *M* phosphate buffer). The  $K_m$  values for amino acid amides are generally higher. The  $K_m$  decreases with increasing hydrophobic character of the side chain.

#### Distribution

In mammalian cells, especially in kidney or liver, there exist at least two different aminopeptidases, one cytoplasmic and one particle bound. They differ strongly in their substrate specificity and their activation by heavy metals. In addition, they are immunologically different. The cytoplasmic enzyme appears to be identical with leucine aminopeptidase and also with the crystalline peptidase of bovine lens.<sup>9</sup>

TABLE III  
AMINO ACID COMPOSITION OF PARTICLE-BOUND AMINOPEPTIDASE

Amino acid	Residues per mole	Amino acid	Residues per mole
Aspartic acid	340	Isoleucine	145
Threonine	107	Leucine	296
Serine	103	Tyrosine	104
Glutamic acid	364	Phenylalanine	144
Proline	197	NH <sub>2</sub>	280
Glycine	127	Lysine	144
Alanine	210	Histidine	60
Valine	165	Arginine	100
Methionine	40	Cysteine	10

#### Functional Amino Acids

The amino acid composition of the enzyme is shown in Table III. Kinetic measurements suggest that some of the tyrosine and histidine side chains, with apparent  $pK$  values of 7.2, 8.7, and 9.7, are involved in catalysis.

At low pH 11<sup>+</sup> is a competitive inhibitor of the ammonium group of the substrate.

Diazonium-*L*-*H*-tetrazole, a substance reacting rapidly with the imidazole side chain of histidine residues in proteins, causes a strong decrease of the enzymatic activity. The inhibition correlates to increasing

<sup>9</sup> H. Hanson, D. Clatter, and H. Hirschke, *Hoppe-Seyler's Z. Physiol. Chem.* 340, 407 (1965).

absorbance at 478 nm, due to the formation of histidine-bisazo-*L*-*H*-tetrazole. Total inhibition corresponds to the reaction of five histidine residues.<sup>10</sup> Wachsmuth described the inactivation of aminopeptidase by iodine, which produces mono and diiodo tyrosine.<sup>11</sup> Fienfer<sup>12</sup> found with tetranitromethane—a high specific reagent for tyrosine—a decrease of enzymatic activity due to formation of nitrotyrosine. The nitrated enzyme is partially active even in a high excess of the reagent.

<sup>10</sup> G. Pfeiderer and U. Fienfer, *FEBS Letters* 4, 205 (1969).

<sup>11</sup> E. D. Wachsmuth, *Biochem. Z.* 346, 446 (1967).

<sup>12</sup> U. Fienfer and G. Pfeiderer, *FEBS Letters* 4, 202 (1969).

#### [35] Aminopeptidase-P

By A. YARON and A. BERGER

#### Assay Method

**Principle.** Aminopeptidase-P is an exopeptidase cleaving the bond between any N-terminal amino acid residue and a following proline residue.<sup>1</sup> The assay is based on the measurement by the acid ninhydrin colorimetric method<sup>2,3</sup> of proline released from the substrate poly-L-proline.

Since the enzyme is an exopeptidase, the rate of appearance of proline is proportional to the concentration of polymer molecules, *c*.

$$c = \frac{\text{mg of polymer}}{\text{ml} \times \text{average molecular weight}} \quad (1)$$

The amount of poly-L-proline necessary to give a solution of known concentration depends therefore on the number average molecular weight of the sample employed. This is determined for a given batch by end group titration.

#### Reagents

Poly-L-proline.<sup>4,5</sup> Commercial poly-L-proline of molecular weight of 5000 to 10,000 is purified and freed from low molecular weight

<sup>1</sup> A. Yaron and D. Mlynar, *Biochem. Biophys. Res. Commun.* 32, 655 (1965).

<sup>2</sup> W. Troll and J. Lindsay, *J. Biol. Chem.* 215, 655 (1955).

<sup>3</sup> S. Surd, A. Berger, and E. Katchalski, *J. Biol. Chem.* 234, 1740 (1959).

<sup>4</sup> A. Berger, J. Kurtz, and E. Katchalski, *J. Am. Chem. Soc.* 76, 5552 (1954).

<sup>5</sup> E. Katchalski, M. Sela, H. I. Silman, and A. Berger, in "The Proteins" Vol. II. (H. Neurath, ed.), p. 405. Academic Press, New York, 1964.

fractions by gel filtration on Sephadex G-25. This procedure is necessary in order to reduce blank values and remove heavy metal impurities.

A  $2.7 \times 90$  cm column of Sephadex G-25 was washed with 0.1 M EDTA (1 liter) followed by double distilled water (2 liters). The sample (500 mg) was applied in 10 ml and eluted under gravity with water (flow rate, 48 ml/hour). The effluent was monitored at 240 nm and 168 ml from the first appearance of absorption were collected. Later fractions showing positive acid ninhydrin reaction were rejected. The solution was lyophilized and dried *in vacuo* over concentrated sulfuric acid at room temperature. The yield was 360 mg.

The number average molecular weight is determined by potentiometric titration of the amino end groups ( $pK_a = 9.0$ ) on a 150-mg sample in 3 ml of 0.1 M NaCl using a 0.1 M NaOH titrant delivered from an Agla microburet. Since the end point is not easily detected, it is convenient to evaluate the number of amino groups from the buffering capacity (i.e., the slope of the titration curve) at pH 9.0:

$$\text{moles of NH in sample} = \frac{d(\text{moles of base})}{dpH} \quad (2)$$

Poly-L-proline stock solution ( $1.66 \times 10^{-3}$  M) is prepared by dissolving the polymer in ice-cold water (poly-L-proline dissolves well in cold water and precipitates on heating). If turbid, the solution is cleared by centrifugation.

Veronal buffer, 0.05 M, pH 8.6. The buffer is passed through a Chelex-100 (analytical grade chelating resin, mesh 50-100, Bio-rad Lab., Richmond, Calif.) column in  $\text{Na}^+$  form, pre-equilibrated with the buffer, and stored at  $4^\circ$ .

Sodium citrate, 0.4 M. The trisodium salt dihydrate is passed through a Chelex-100 column in  $\text{Na}^+$  form, pre-equilibrated with the sodium citrate solution, and stored at  $4^\circ$ .

Manganous chloride, 0.1 M. A 1 M solution of  $\text{MnCl}_2$  in water (500 ml) is passed through a 25-ml Chelex-100 column in  $\text{Na}^+$  form. The first 100 ml of the effluent are discarded. The manganese concentration is determined by complexometric titration with Versene, using bromochrome black as the indicator. The solution is diluted to 0.1 M with double distilled (metal-free) water.

Sodium hydroxide, 0.1 M. 0.1 M sodium hydroxide is passed through a Chelex-100 column in  $\text{Na}^+$  form.

EDTA (sodium salt), 0.01 M

Ninhydrin reagent. Ninhydrin (3 g) is dissolved in a mixture of

glacial acetic acid (60 ml) and phosphoric acid (6 M, 40 ml) by warming at  $70^\circ$ .

Glacial acetic acid

Enzyme. The enzyme preparation (in 0.05 M acetate buffer pH 6.5, or 0.1 M phosphate buffer, pH 7.0, about 15 units per milliliter) can be stored at  $4^\circ$  or frozen for several months.

Mn-citrate reagent. This reagent is prepared fresh before the assay by mixing 2.5 ml 0.05 M Veronal buffer, 0.5 ml of 0.4 M sodium citrate, 0.5 ml of 0.1 M manganous chloride, and 0.5 ml of 0.1 M sodium hydroxide.

*Procedure*

To a test tube is added 0.025 ml of poly-L-proline stock solution, 10  $\mu$ l of 0.01 M Versene, 0.75 ml of Veronal buffer, and 0.2 ml of Mn-citrate reagent. The solution is placed into a  $40^\circ$  water bath, and 15  $\mu$ l of enzyme solution (suitably diluted to produce 5-20  $\mu$ g proline in 30 minutes) is added. After 30 minutes, the reaction is stopped by adding 2.5 ml of ninhydrin reagent and the solution cooled with tap water. At this stage samples can be stored for several hours. For determination of proline formed during the hydrolysis, 2.5 ml of glacial acetic acid is added and the solution heated at  $100^\circ$  for 30 minutes. After cooling, the intensity of the red color is measured in a Klett-Summerson photoelectric colorimeter with a filter No. 52. The amount of proline formed is calculated from a calibration curve constructed with known amounts of proline.

*Definition of Unit and Specific Activity.* One unit of activity is defined as the amount of enzyme which produces 1 mg proline per milliliter of incubation solution under the conditions of the above-described assay.

Since the low concentration of poly-L-proline in the assay solution does not correspond to the saturation region of the substrate concentration curve, the unit defined depends on the poly-L-proline concentration. The assay is also very sensitive to the purity of reagents which thus affects the unit as defined.

The specific activity is expressed in units per milligram of protein.

It should be noted that enzyme activity is quite proportional to enzyme concentration in the range from zero to about 20 millimoles per milliliter. At higher concentration deviation from linearity is pronounced, due to association (see below).

*Assay of Enzyme in Tissue Extracts.* Aminopeptidase-P is not the only enzyme-producing proline from poly-L-proline. Proliminopeptidase<sup>3,9</sup> is also known to cause similar hydrolysis. The differentiation

<sup>9</sup>S. Sarid, A. Berger, and E. Katchalski, *J. Biol. Chem.* 237, 2207 (1962).



between the two enzymes is based on their different specificity. The sequential polymers poly-(Pro-Gly-Pro) and poly-(Gly-Pro-Pro) can be used for the differentiation, the former being readily hydrolyzed by proliniminopeptidase, the latter by aminopeptidase-P. Tissue extracts when dialyzed against buffers contain very little material reacting to the acid ninhydrin test and can therefore be easily assayed by the described procedure. Bradykinin may be used as an alternative substrate for aminopeptidase-P. In this case 1 mole of arginine and 1 mole of proline are released.

#### Purification Procedure

Because the enzyme is very sensitive to heavy metal contaminants, all buffers and salt solutions are passed through columns of Chelex-100 (analytical grade chelating resin, mesh 50-100, Biorad Lab., Richmond, Calif.) pre-equilibrated with the reagent. Metal-free water is used throughout.

The enzyme is isolated from *Escherichia coli* (wild type) and purified 850 times. The enzyme is unstable to lyophilization, but can be kept frozen for several months without loss of activity. The procedure is described for a 1300-g batch of wet cells and is performed at 4°.

**Preparation of Cell-Free Extract.** Mass cultures of *Escherichia coli* strain B are grown in lots of 14 liters with aeration at 37° on yeast extract (1.0%), K<sub>2</sub>HPO<sub>4</sub> (2.18%), KH<sub>2</sub>PO<sub>4</sub> (1.70%), and glucose (1.0%). The cells are harvested after 5 hours in a Sharples ultracentrifuge (4 g wet cells per liter). The wet cells are kept frozen at -20° until a sufficient amount is collected by repeated growing of bacteria.

The frozen mass is dispersed at 4° by occasional shaking during 2 days in a 0.9% potassium chloride solution (4.6 ml/g).

The cells are then ruptured by passing the cold (4°) suspension through a Manton-Gaulin homogenizer (Model 15 M Everett, Mass.) at 4500 psi. (Changing the pressure to 3000 psi or to 6000 psi resulted in a specific activity lower by 17%. Repeating the homogenization did not increase the yield.)

Cell debris is removed by centrifugation for 30 minutes in a Sorvall Superspeed RC-2 automatic centrifuge with the GSA-rotor at 23,000 g at 0°-2°. The extract can be stored frozen at -20° for several weeks without loss of activity.

**Heat Precipitation.** The cell-free extract is warmed to room temperature (24°) with tapwater and heat precipitated by passing the extract under gravity through a spiral glass tubing of 0.50 cm internal diameter and 125 ml capacity immersed in a water bath kept at 53°.

The extract is passed at a flow rate of 200 ml/minute and emerges at a temperature of 50°. Fractions of 400 ml are collected in polyethylene 0.5-liter bottles preheated to 50°. Each fraction is then kept for 15 minutes in a 50° water bath, cooled in an ice bath, and stored at 4°.

In preliminary experiments it was shown that the enzyme activity at 50° was constant for 20 minutes. The specific activity after 5, 10, 16, and 20 minutes was 0.084, 0.086, 0.094, and 0.094, respectively. At 60° a sample of 1095 units/ml contained after 3, 7, 11, and 15 minutes 860, 685, 520, and 470 units/ml, respectively.

**Ammonium Sulfate Precipitation.** A saturated ammonium sulfate solution is neutralized to pH 7.0 by adding solid potassium carbonate (approx. 1 g per 1 liter). The solution is filtered if necessary and passed at a 700 ml/hour flow rate through a Chelex-100 column in NH<sub>4</sub><sup>+</sup>-form (3.0 × 45 cm) equilibrated with the saturated ammonium sulfate solution. To the metal-free solution was added sodium citrate (Na<sub>3</sub>C<sub>6</sub>H<sub>5</sub>O<sub>7</sub> · 2 H<sub>2</sub>O, 0.59 g/liter) and the solution was stored at 4°, where the excess of ammonium sulfate crystallizes out and the supernatant is used for the fractionation procedure.

Saturated ammonium sulfate solution is added at 2° to the extract containing the precipitated proteins (787 ml ammonium sulfate solution per each liter of the extract). The clear supernatant is obtained by centrifugation and mixed with another portion of saturated ammonium sulfate (600 ml ammonium sulfate solution per each liter of the supernatant). The precipitate formed is isolated by centrifugation and dissolved in 0.05 M sodium acetate, pH 5.6. (For volumes used to dissolve the precipitate, see Table I.) The solution obtained loses 12% of its activity in 10 days when kept frozen at -20°, or 23% when kept at 4° for the same period.

In preliminary experiments it was found that reversing of the two purification steps, namely precipitating with ammonium sulfate first and heat precipitating thereafter, resulted in appreciable loss of activity. No advantage in terms of yield or purification was gained by removing the denatured proteins prior to the precipitation by ammonium sulfate.

**Acetone Precipitation.** Cold acetone (850 ml) is added during 20 minutes at -3° with stirring to the solution from the previous purification step (1000 ml). The formed precipitate is isolated with the aid of a Sorvall Superspeed RC-2 automatic refrigerated centrifuge (11,000 rpm), rotor GSA. The precipitate is well dispersed in 0.05 M sodium acetate, pH 5.6 (1000 ml) at 0° and extracted for 30 minutes. The undissolved material is removed by centrifugation and the supernatant is frozen and stored at -20°. No loss of activity was observed after 3 months of storage.

TABLE I  
PURIFICATION OF AMINOPEPTIDASE-P<sup>a</sup>

Procedure	Volume (ml)	Activity <sup>b</sup> (units/ml)	Total units	Protein <sup>c</sup> (mg/ml)	Specific activity (units/mg)	Yield (%)	Purification factor
Cell-free extract	6,300	2.3	14,500	16.9	0.136	100	1
Heat precipitation	6,300	2.23	14,100	11.3	0.198	96.7	1.45
Ammonium sulfate fractionation	1,000	10.5	10,500	22.6	0.465	72	3.4
Acetone fractionation	1,000	9.5	9,500	3.78	2.52	65	18.4
Ca-phosphate gel	2,000	4.03	8,070	0.23	17.3	56	127
DEAE-cellulose	29	197	5,720	4.62	42.5	39.3	313
Gel filtration	107	42.7	4,560	0.37	116	31.4	855

<sup>a</sup> Figures are given for 1300 g frozen wet cells of *E. coli* B.

<sup>b</sup> The activity was determined as described in the text. One unit of activity is defined as the amount of enzyme which produces 1 mg proline per milliliter of incubation solution under the conditions of the above-described assay.

<sup>c</sup> Protein concentration was determined by the method of Lowry.<sup>9</sup> Bovine serum albumin was used as standard.

**Adsorption on Calcium Phosphate.** A calcium phosphate gel suspension in water (22 mg/ml) is prepared according to Keilin and Hartree.<sup>7</sup> The suspension (30 ml) is added to the enzyme solution obtained in the previous step (1000 ml) and stirred at 4° for 10 minutes. The solid is removed by centrifugation and another portion of the gel suspension (210 ml) is added to the supernatant and mixed for 15 minutes. Both portions of the gel are resuspended in a solution of 1 M KCl in 0.05 M sodium acetate, pH 5.6 (1000 ml), mixed for 15 minutes and the supernatant discarded after centrifugation. The gel sediment is then extracted with two 1-liter portions of 0.05 M sodium phosphate buffer, pH 6.0 (1000 ml), for 25 minutes. The extract can be stored at 4°.

**Fractionation on DEAE-Cellulose.** The solution from the previous step (2000 ml) is applied under gravity at a flow rate of 72 ml/hour to a DEAE-cellulose column (1.7 × 43 cm) which was previously equilibrated with 0.05 M sodium acetate buffer, pH 5.6, containing 0.002 M sodium citrate. The column is washed with the same buffer (125 ml) followed by a solution of 0.05 M KCl in 0.1 M sodium acetate, pH 5.6, containing 0.002 M sodium citrate (500 ml). The adsorbed activity is finally eluted with 0.4 M ammonium sulfate in 0.1 M sodium acetate, pH 5.6, containing 0.002 M sodium citrate at a 30 ml/hour flow rate. The activity started to appear after 60 ml and emerged in a 29-ml volume.

**Gel Filtration on Sephadex G-200.** The solution obtained in the previous step (29 ml) is applied to a Sephadex G-200 (particle size 40–120 μ, Pharmacia, Uppsala, Sweden) column (3.8 × 191 cm) equilibrated with 0.1 M sodium acetate, pH 5.6, containing 0.002 M sodium citrate. The same buffer is used for elution at a 10 ml/hour flow rate. The active fraction starts to appear soon after the void volume and emerges in an approximately 150-ml volume. Fractions of about 15 ml are collected and checked for specific activity. Most of the enzyme (80%) is eluted in fractions having constant specific activity (116 units per milligram). This solution can be kept frozen for more than a year.

### Properties

**Stability.** The enzyme is stable when kept either in 0.1 M sodium acetate buffer, pH 5.6, containing  $2 \times 10^{-3}$  M sodium citrate or in 0.1 M phosphate buffer, pH 7.0, containing 0.05 M EDTA. It loses activity on lyophilization. However, the enzyme can be conveniently concentrated by pressure filtration through a Diaflo ultrafiltration membrane TMF-2, (solute cutoff 1000 MW, Amicon, Lexington, Mass.). Alternatively, the enzyme can be applied to a DEAE-cellulose column and eluted at high

<sup>7</sup> D. Keilin and R. F. Hartree, *Proc. Roy. Soc. (London) Ser. B* 124, 397 (1938).

ionic strengths. In a representative run, an enzyme solution obtained from the last purification step (46 ml) was applied to a 10 ml DEAE-cellulose column equilibrated with 0.05 *M* sodium acetate buffer, pH 5.6,  $2 \times 10^{-3}$  *M* in sodium citrate and eluted with 0.4 *M* ammonium sulfate in 0.1 *M* sodium acetate, pH 5.6,  $2 \times 10^{-3}$  *M* in sodium citrate. The activity (75%) emerged in a 2-ml volume. The salt can be removed by dialysis against the acetate or phosphate buffer containing EDTA. Membranes should be washed with EDTA solution.

**Purity and Physical Properties.** The protein composition of the enzyme preparations obtained after the different purification steps was followed by polyacrylamide gel electrophoresis.<sup>8</sup> After the last purification step (factor of purification: 860) a single band was observed.<sup>1</sup>

**Absorption Spectrum.** The enzyme displayed a typical protein absorption peak at 278 nm and a 1.8 ratio of absorbance at 278 and 260 nm, respectively. The extinction was  $OD_{260} = 1.03$  (1 cm) at a concentration of 1 mg/ml (determined from the Kjeldahl nitrogen using a factor of 6.25). The color yield in the Lowry method<sup>9</sup> is the same as for bovine serum albumin.

**Sedimentation and Diffusion Coefficients.** These coefficients of the pure enzyme were measured in 0.407 *M* ammonium sulfate, 0.1 *M* in Na-acetate, pH 5.6, containing 0.002 *M* sodium citrate. The enzyme sedimented as a single symmetric boundary in the ultracentrifuge. From the sedimentation coefficient  $s_{0,w}^0 = 9.1$  S, obtained after extrapolation to zero concentration, the diffusion coefficient  $D_{20,w}^0 = 4.4 \times 10^{-7}$  cm<sup>2</sup>/sec, and an assumed partial specific volume of 0.74, a molecular weight of 205,000 was calculated. A sedimentation equilibrium run with a 0.15% solution of the enzyme in the same solvent evaluated by the Yphantis midpoint method yielded a molecular weight of 230,000.

**Amino Acid Analysis.** The amino acid composition of aminopeptidase-P is recorded in Table II. The protein obtained after the last gel filtration purification step was hydrolyzed with 6 *N* HCl in evacuated sealed tubes at 100° for 24, 48, and 72 hours. Amino acid analysis was performed with an automatic amino acid analyzer. The values for serine, threonine, and tyrosine were corrected for decomposition during hydrolysis by extrapolating to zero time of hydrolysis. Also, the amide nitrogen was calculated from the ammonia content of the 24, 48, and 72-hour hydrolyzates after extrapolation to zero time. Valine and isoleucine were incompletely released at 24 hours, and for that reason their values were calculated from the 48- and 72-hour hydrolyzates. No cystine was found

<sup>8</sup> B. J. Davis, *Ann. N.Y. Acad. Sci.* 121, 404 (1964).

<sup>9</sup> O. H. Lowry, N. J. Rosebrough, A. L. Farr, and R. J. Randall, *J. Biol. Chem.* 193, 265 (1951).

TABLE II  
AMINO ACID COMPOSITION OF AMINOPEPTIDASE-P

Amino acid	Micromoles amino acid per 100 micromoles N
Asp	5.45
Thr	2.83
Ser	3.20
Glu	8.60
Pro	1.93
Gly	4.76
Ala	5.12
Half-cys	—
Val	4.52
Met	1.26
Ile	3.90
Leu	5.54
Tyr	1.88
Phe	2.15
Trp	0.47
Lys	2.10
His	2.08
Ammonia	5.80
Arg	4.50
Cys-SO <sub>3</sub> H	0.50 <sup>a</sup>
Cysteine	0.60

<sup>a</sup> Determination of both cystine plus cysteine as cysteic acid was performed by performic oxidation and analysis according to Moore.<sup>10</sup>

<sup>b</sup> Determination of —SH groups was performed by the Ellman method<sup>11</sup> in presence of 1% sodium dodecylsulfate. The number of cysteic acid residues per 100 micromoles N was calculated from the average of two determinations of cysteic acid, and the average molar ratio of alanine, leucine, glutamic acid, and aspartic acid to cysteic acid was used to express the number of cysteic acid micromoles per 100 micromoles of nitrogen.

by the amino acid analysis of the hydrolyzates. Cysteic acid was quantitatively determined after performic acid oxidation according to Moore.<sup>10</sup> Sulfhydryl content in the intact protein was determined by the Ellman procedure<sup>11</sup> in presence of 1.0% sodium dodecylsulfate and 10<sup>-4</sup> *M* EDTA. Tryptophan was determined spectrophotometrically.<sup>12</sup> The amino acid analysis accounts for 87% of the total nitrogen.

**pH Profile.** The dependence of activity on pH determined in 0.05 *M* Veronal buffer at three Mn<sup>2+</sup> concentrations is given in Fig. 1. The bell-shaped curve shows a maximum at pH 8.6.

<sup>10</sup> S. Moore, *J. Biol. Chem.* 238, 255 (1963).

<sup>11</sup> G. L. Ellman, *Arch. Biochem. Biophys.* 82, 70 (1959).

<sup>12</sup> T. W. Goodwin and R. A. Morton, *Biochem. J.* 40, 628 (1946).

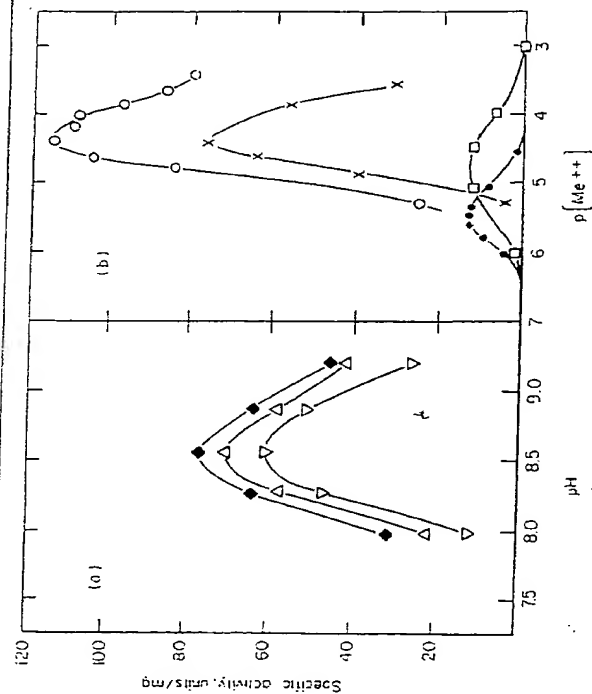


FIG. 1. (a) The dependence of specific activity on pH in 0.05 *M* Veronal buffer.  $Mn^{2+}$  concentrations: (♦)  $3.7 \times 10^{-5} M$ , (Δ)  $5.0 \times 10^{-4}$ , (▽)  $2.5 \times 10^{-3}$ . (b) The dependence of specific activity on metal ion concentration. Metal added as (X)  $MnCl_2$ , (O)  $Mn^{2+}$  citrate-metallobuffer system, (●)  $CoCl_2$ , (□)  $CdCl_2$ .<sup>12</sup>

**Metal Ion Requirement.** Exhaustive dialysis of the enzyme against buffers containing EDTA leads to a completely inactive preparation. Activation can be achieved by removing the EDTA by dialysis and adding  $Mn^{2+}$ ,  $Co^{2+}$ ,  $Cd^{2+}$ , or  $Ni^{2+}$ .<sup>13</sup> The dependence of specific activity on the negative log of the concentration of the metal ions is given in Fig. 1. Also for the metals bell-shaped curves are obtained. The highest activity was achieved with  $Mn^{2+}$ , although  $Co^{2+}$  activates at a ten times lower concentration. A quite sharp optimum in activity occurs at a  $Mn^{2+}$  concentration of  $3.7 \times 10^{-5} M$ . This maximum was observed at all pH values at which activity could be tested (7.0–9.2). The pH of highest activity was always 8.6.

The required concentration of free  $Mn^{2+}$  in the assay solution is reached by using  $MnCl_2$ -sodium citrate as a metallobuffer.<sup>14</sup> Incorporation of citrate in the assay solution was found also to protect the enzyme against the inhibitory effects of traces of heavy metals.

<sup>12</sup> R. Granath, Ph.D. thesis, Feinberg Graduate School, The Weizmann Institute of Science, Rehovot, Israel, to be published.

<sup>13</sup> J. Raafaub, in "Methods of Biochemical Analysis" (D. Gluck, ed.), Vol. 3, p. 301. Wiley (Interscience), New York, 1956.

**Specificity.** Aminopeptidase-P acts on polypeptides, cleaving the peptide bonds formed between the carboxyl of an N-terminal amino acid residue and the secondary amine of a proline residue:  $H_2N-^1Pro-^2Phe-^3OH$ . The following low molecular weight peptides are hydrolyzed:  $L-prolyl-L-prolyl-L-alanine$ ,  $glycyl-L-prolyl-L-glycine$ ,  $glycyl-L-proline$ ,  $L-valyl-L-proline$ ,  $L-alanyl-L-proline$ , and  $L-prolyl-L-proline$ . The dipeptide  $glycyl-L-proline$  is digested considerably slower than higher peptides and the same applies to  $L-valyl-L-proline$  and  $L-alanyl-L-proline$ . Bradykinin ( $Arg-Pro-Gly-Phe-Ser-Pro-Phe-Arg$ ) is digested rapidly (enzyme concentration 4.4  $\mu g/ml$ ), one arginine being released per one bradykinin molecule in less than 5 minutes and the following proline residue is released within 1 hour (80% in 30 minutes). No additional splits were observed after 24 hours. Reduced and carboxymethylated papain, which has the N-terminal sequence  $Ile-Pro-Glu-Tyr-Val \dots$ , was digested rapidly. At an enzyme concentration of 1.3  $\mu g/ml$ , 1 mole of isoleucine was liberated within 1 hour (substrate  $10^{-4} M$ ). No other amino acids were released. The terminal amino group seems to be essential, as dinitrophenyl  $poly-L-proline$  is resistant to hydrolysis, in contrast to the rapidly hydrolyzed  $poly-L-proline$ . Hydroxyproline cannot be substituted for proline in the substrates of aminopeptidase-P, since  $poly-L-hydroxyproline$  and  $L-prolyl-L-hydroxyprolyl-L-alanine$  are not digested. Substrates of leucine aminopeptidase such as  $L-leucyl-L-serine$  are not digested, neither are peptides with an N-terminal  $L-proline$  residue when not followed by another  $L-prolyl$ , i.e.,  $L-prolylglycine$ ,  $L-prolyl-L-phenylalanyl-L-lysine$ , or  $salmine$  which are substrates of proline iminopeptidase.<sup>3,6</sup> are not hydrolyzed and were found to inhibit competitively the hydrolysis of  $poly-L-proline$  by aminopeptidase.

Because of the specificity described above, aminopeptidase-P may be expected to find useful application in studies of protein structure mainly in proline-rich proteins. It is pertinent to note that leucineaminopeptidase is capable of removing amino acid residues from a polypeptide until the residue preceding proline. Aminopeptidase-P is capable of cleaving this residue, revealing an N-terminal proline, which in turn can be removed by proline iminopeptidase.

**Kinetic Parameters.** DEPENDENCE OF SPECIFIC ACTIVITY ON ENZYME CONCENTRATION. It was observed that enzyme activity does not increase linearly with enzyme concentration (see Fig. 2). Since in gel filtration experiments it was observed<sup>15</sup> that the apparent molecular weight of the enzyme decreases from about 200,000 at 25  $\mu g/ml$  (in the sample applied) to about 100,000 at 1.0  $\mu g/ml$ , it was tentatively assumed that only the 100,000 MW species ( $M$ ) is enzymatically active, whereas the 200,000 MW species ( $D$ ) is inactive. Assuming the dissociation equilibrium

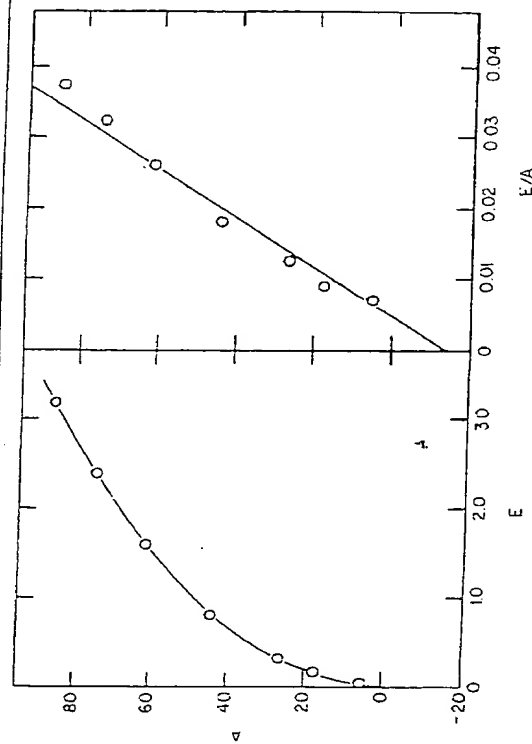


FIG. 2. The dependence of activity  $A$  (in enzyme units), on enzyme concentration  $E$  (in  $\mu\text{g/ml}$ ). From the intercept on the  $E/A$  coordinate of the  $A$  vs.  $E/A$  plot, a maximum specific activity of 230 units per milligram protein is obtained. The dissociation constant calculated from the two intercepts is  $K = 0.1 \mu\text{g/ml}$  or  $10^{-3} M$  (based on a molecular weight of  $10^5$ ).

where

$$I = 2 M$$

$$K = M^2/I$$

a plot of activity vs. the reciprocal specific activity should be linear.

If  $E$  is the total enzyme concentration (as monomer), it follows that  $K = 2 M^2/(E - M)$ . Taking the activity as  $A = \alpha dI$ , where  $\alpha$  is a constant depending on the definition of the unit of activity, then  $A = (\alpha^2 KE/2A) - (\alpha K/2)$ ,  $E/A$  being the reciprocal specific activity.

The intercept ( $I'$ ) on the reciprocal specific activity coordinate gives the maximum specific activity and the product  $2I'$  (where  $I$  is the intercept on the activity coordinate) gives the dissociation constant. This relationship was indeed observed (see Fig. 2).<sup>13</sup>

MICHAELIS-MENTEN PARAMETERS. The parameters  $\bar{K}_m$  ( $=1/K_m$ ) and  $k_{cat}$ , obtained from Lineweaver-Burk plots using initial rates, are given in Table III. The plots were linear in the substrate concentration ranges investigated ( $10^{-6}$  to  $10^{-3} M$  for poly-L-proline and  $10^{-3}$  to  $10^{-2} M$  for L-prolyl-L-prolyl-L-alanine).

The very pronounced substrate specificity for L-proline indicates the presence of a specific binding site for a proline residue in the active site

TABLE III  
KINETIC PARAMETERS

Substrate or competitive inhibitor	$\bar{K}_m$ ( $M^{-1}$ )	$\bar{K}_i^a$ ( $M^{-1}$ )	$k_3^b$ ( $\text{sec}^{-1}$ )
Poly-L-proline (MW 6000) <sup>c</sup>	11300	—	105
H-Pro-Pro-Ala-OH <sup>d</sup>	870	—	1210
H-Pro-Phe-Lys-OH <sup>e</sup>	—	8500	—
H-Pro-Phe-OH <sup>e</sup>	—	13300	—
H-Pro-Ala-OH <sup>e</sup>	—	1000	—
H-Ala-Phe-Lys-OH <sup>e</sup>	—	<500	—

<sup>a</sup> Obtained from Lineweaver-Burk plots. The composition of the reaction mixture was that of the standard assay; substrate Pro-Pro-Ala  $10^{-3}$  to  $10^{-4} M$ .  
<sup>b</sup> Assumed MW 100,000.

<sup>c</sup> Enzyme concentration  $0.3 \mu\text{g/ml}$ .

<sup>d</sup> Enzyme concentration  $0.06 \mu\text{g/ml}$ .

<sup>e</sup> Enzyme concentration  $0.057 \mu\text{g/ml}$ .

<sup>f</sup> No inhibition at  $2.3 \times 10^{-3} M$  peptide.

of the enzyme. Product inhibition by peptides with N-terminal proline could therefore be expected. Indeed, it was found that L-prolyl-L-phenyl-alanine is a strong competitive inhibitor. By comparison of the reciprocal inhibition constants  $\bar{K}_i$  ( $=1/K_i$ ) in Table III, it can be seen that most of the binding energy is contributed by the proline residue. When the residue next to proline is phenylalanine, about ten times stronger inhibition is observed than in the case of L-prolyl-L-alanine. This indicates a considerable contribution of the aromatic residue to the binding energy of the inhibitor.

**Occurrence.** Occurrence in the microsome fraction of swine kidney of an aminopeptidase having a specificity similar to the bacterial aminopeptidase-P was reported by Nordwig and Dehm.<sup>15</sup>

A substrate specificity similar to that of aminopeptidase-P was repeatedly claimed<sup>16-18</sup> for the dipeptidase proliadase.<sup>20</sup> However, pure proliadase was shown to digest specifically dipeptides with a C-terminal proline or hydroxyproline, whereas the tripeptide Gly-Pro-Gly was not digested.<sup>20</sup> In contrast, aminopeptidase-P digests Gly-Pro-Gly (and bradykinin) much more readily than the dipeptide Gly-Pro.

The observations that proliadase can to some extent cleave glycine

<sup>15</sup> A. Nordwig and P. Dehm, *Biochim. Biophys. Acta* 160, 293 (1968).

<sup>16</sup> A. Light and J. Greenberg, *J. Biol. Chem.* 240, 258 (1965).

<sup>17</sup> R. L. Hill and W. R. Schmidt, *J. Biol. Chem.* 237, 389 (1962).

<sup>18</sup> R. Frater, A. Light, and E. L. Smith, *J. Biol. Chem.* 240, 253 (1965).

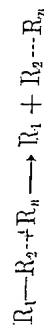
<sup>19</sup> C. Nolan and E. Smith, *J. Biol. Chem.* 237, 453 (1962).

<sup>20</sup> N. C. Davis and E. L. Smith, *J. Biol. Chem.* 234, 261 (1957).

from Gly·Pro·Leu,<sup>17</sup> isoleucine from denatured papain,<sup>18</sup> glutamine from GluNH<sub>2</sub>·Pro·Ser·Val·Val·Leu,<sup>14</sup> and lysine from a peptide Lys·Pro·Arg·Glu . . . ,<sup>19</sup> seem to indicate the presence of aminopeptidase-P in the prolidase preparations used, all of which were of low degree of purity.

### [36] Brain Aminopeptidase Hydrolyzing Leucylglycylglycine and Similar Substrates

By NEXVILLE MARKS and ABEL LAJTHA



Intracellular α-aminopeptidase amino acid hydrolases (EC 3.4.1) are widely distributed in animal tissues but have been studied in brain only recently.<sup>2-6</sup>

Peptide hydrolases as such are not clearly defined in the literature, but the purified brain aminopeptidase described below appears to be distinct from the enzymes that hydrolyze L-leucyl peptides (leucine aminopeptidase, EC 3.4.1.2),<sup>7</sup> aminoacyl oligopeptides (aminopeptidase, EC 3.4.1.2),<sup>8</sup> and amino acid dipeptides (aminotripeptidase, EC 3.4.1.2).<sup>9</sup> All tissues appear to contain a complex mixture of peptide hydrolases of varying specificity. Brain aminopeptidase is a stable enzyme extracted from the soluble supernatant of whole pig brain and defined by its chromatographic profile on DEAE-cellulose, its specificity against tripeptides such as LLL<sup>10</sup> and LGG, and by its unique cleavage of some alanyl oligopeptides.

#### Assay Methods

Two different methods are described: (1) a microassay procedure for monitoring enzyme purification and the rapid screening of materials for potential substrate activity; and (2) a quantitative procedure for the

<sup>1</sup> N. Marks, R. K. Datta, and A. Lajtha, *J. Biol. Chem.* 243, 2882 (1968).

<sup>2</sup> R. K. Datta, N. Marks, and A. Lajtha, *Federation Proc.* 17, 302 (1967).

<sup>3</sup> N. Marks, *Intern. Rev. Neurobiol.* 11, 57 (1968).

<sup>4</sup> A. S. Brecher and R. E. Sobel, *Biochem. J.* 105, 641 (1967).

<sup>5</sup> N. Marks in "Handbook of Neurochemistry" (A. Lajtha, ed.), Vol. 3, p. 133. Plenum Press, New York, 1970.

<sup>6</sup> Abbreviations used: amino acids in peptide linkage are according to the single letter code of IUPAC-IUB (*Biochem. J.* 113, 1 (1969)). A, alanyl; L, leucyl; G, glycyl; Y, tyrosine. —βNA denotes the naphthylamide moiety of the arylamide substrate. All amino acids unless defined otherwise are of the L-configuration.

isolation of the degradation products themselves for purposes of determining the stoichiometry of peptide breakdown.

**Principle.** The chief disadvantage of the standard quantitative ninhydrin procedure is the relatively high background of the substrate compared to the liberated products. This method can be modified to reduce E (the molar extinction coefficient) for di- and tripeptides (the substrates) compared to the liberated amino acids. A comparison of E for peptides used in this report based on the modified procedures of Yemm and Cocking<sup>6</sup> and Matheson and Tattrie<sup>7</sup> is given in Table I.

TABLE I  
COMPARISON OF E VALUES WITH DIFFERENT NINHYDRIN REAGENTS<sup>a</sup>

Substrate	E Values	
	Ninhydrin reagent (modified)	Ninhydrin hydriindantin reagent
Leu-	1.95	2.15
Ala-	1.79	2.30
Gly-	2.01	2.17
Leu-Gly	0.35	2.47
Leu-Gly-Gly	0.38	2.05
Ala-Ala	0.35	4.10
Gly-Gly	1.39	2.04
Gly <sub>1</sub>	1.13	1.91
Gly-Leu	1.44	2.18

<sup>a</sup> Data derived from Matheson and Tattrie.<sup>7</sup>

Stoichiometric studies of peptide breakdown require the isolation of degradation products. Paper chromatographic methods have been suggested<sup>1,8</sup> but the losses after elution and the unpredictability of color yield are adverse factors. The method of choice is the use of the standard amino acid analyzer as described below.

#### Microassay Procedure

##### Reagents

Citrate buffer, 0.2 M, pH 5.0 (21.0 g C<sub>6</sub>H<sub>5</sub>O<sub>7</sub>·H<sub>2</sub>O dissolved in 200 ml water + 1 N NaOH diluted to 500 ml)

NaCN, 1 mM (4.9 mg NaCN in 100 ml), KCN can be substituted.

Store in a glass-stoppered bottle. Stable 6 months at 4°.

<sup>6</sup> E. W. Yemm and E. C. Cocking, *Analyst* 80, 207, (1955).

<sup>7</sup> A. T. Matheson and B. L. Tattrie, *Can. J. Biochem.* 42, 95<sup>16</sup> (1964).

<sup>8</sup> S. Ellis and J. M. Nuenke, *J. Biol. Chem.* 242, 4623 (1967).

**This Page is Inserted by IFW Indexing and Scanning  
Operations and is not part of the Official Record**

**BEST AVAILABLE IMAGES**

Defective images within this document are accurate representations of the original documents submitted by the applicant.

Defects in the images include but are not limited to the items checked:

- ☐ **BLACK BORDERS**
- ☐ **IMAGE CUT OFF AT TOP, BOTTOM OR SIDES**
- ☐ **FADED TEXT OR DRAWING**
- ☐ **BLURRED OR ILLEGIBLE TEXT OR DRAWING**
- ☐ **SKEWED/SLANTED IMAGES**
- ☐ **COLOR OR BLACK AND WHITE PHOTOGRAPHS**
- ☐ **GRAY SCALE DOCUMENTS**
- ☐ **LINES OR MARKS ON ORIGINAL DOCUMENT**
- ☐ **REFERENCE(S) OR EXHIBIT(S) SUBMITTED ARE POOR QUALITY**
- ☐ **OTHER:** \_\_\_\_\_

**IMAGES ARE BEST AVAILABLE COPY.**

**As rescanning these documents will not correct the image problems checked, please do not report these problems to the IFW Image Problem Mailbox.**